Vol 18 No 7, July 2009
1674-1056/2009/18(07)/2709-10

Chinese Physics B

© 2009 Chin. Phys. Soc.
and IOP Publishing Ltd

Density functional study of Al-doped Au clusters*

Zhao Li-Xia(赵丽霞)†, Feng Xiao-Juan(冯晓娟), Cao Ting-Ting(曹廷廷), Liang Xiao(梁 晓), and Luo You-Hua(罗有华)

Department of Physics, East China University of Science and Technology, Shanghai 200237, *China*

(Received 21 July 2008; revised manuscript received 21 January 2009)

The equilibrium geometries and electronic properties of Au_nAl, up to $n = 13$, have been systematically investigated using the density functional theory. The results show that, for the Au_nAl clusters, two patterns are identified. Pattern one ($n = 2$, 3, 8), the lowest-energy geometries prefer two-dimensional structures. Pattern two ($n = 4 - 7$, 9–13), the lowest-energy geometries prefer three-dimensional structures. According to the analysis of the binding energy and the fragmentation energy, Au_nAl clusters with odd n are found to be more stable than those with even n. The same trend of alternation can be illuminated according to the computational results in the HOMO–LUMO gap, the ionization potential, and the electron affinities. The Al atom not only changes the structures of pure gold clusters, but also enhances their stabilities. NBO analysis indicates 6s orbital of Au atom hybridizes with 3p orbital of Al atom.

Keywords: Au_nAl clusters, equilibrium geometries, electronic properties, NBO analysis
PACC: 3120A, 3640, 3640B

1. Introduction

During the last decade, gold clusters have received widespread attention due to their potential applications in catalysis, medical sciences, sensors and so on.[1−4] Many experimental and theoretical efforts hitherto have been devoted to structures, stabilities and properties of gold clusters.[5−17] In order to enhance the stability of gold clusters and improve their chemical activities, many studies have been performed on doping gold clusters.[18−37] For example, using an *ab initio* molecular dynamics simulation method, Majumder *et al* have observed the structure and electronic properties of Au_nSi ($n = 1 - 8$)[38] and Au_nS ($n = 2 - 10$)[39] clusters to understand the influence of the doping atom on the geometrical and electronic structures of free gold clusters. Employing first-principles methods, Yuan *et al* [40] reported the ground state geometric and electronic structures of Au_nM ($n \leq 7$, M=Ni, Pd, Pt) clusters and found the dopant atoms markedly change the geometric and electronic properties of gold clusters. Furthermore, Chen and Yan studied the stability and structures of Au_nTi ($n = 2 - 16$).[41] Wang *et al* studied the structures and electronic properties of Au_nCu ($n = 2 - 9$).[42]

In recent years, increasing effort has been devoted to the study of the geometric and electronic properties of nanoclusters composed of Au and Al atoms, both for theoretical reasons and for their potential applications in the emerging field of nanotechnology. In 1999, Bouwen and his co-workers[43] produced bimetallic Au_nAl using a dual-target dual-laser vapourization source. In this year, Heinebrodt *et al*[44] have studied the bimetallic cluster ions of composition Au_nAl^+ using time-of-flight mass spectrometry. Very recently, Majumder *et al* [45] performed geometry optimizations and electronic property calculations of Au_5Al cluster.

It is obvious that the existent theoretical study on Au_nAl clusters is not sufficient, and the detailed structural and electronic properties of Au_nAl ($n > 5$) clusters are still unclear. So far, there are no systematical first principles calculations on Au_nAl clusters. Therefore, it is desirable to extend the study of Au_nAl clusters to larger size so as to obtain a comprehensive understanding of their structures and properties. In order to give further insight into the Au_nAl clusters system, in this paper, we perform first-principle calculations for atomic structures and electronic properties of these clusters. In Section 2, we briefly describe computational methods, and finally, our results and discussions are presented.

*Project supported in part by the National Natural Science Foundation of China (Grant No 10174086) and the Foundation for the research starting of East China University of Science and Technology (Grant No YK0142109).
†E-mail: zlx@ecust.edu.cn

2. Computational details

Based on the PW91PW91 functional[46] and CEP-121G[47] basis set, the geometry optimizations of small Au_nAl clusters with $n \leq 13$ are carried out by solving the Kohn–Sham equation[48] in the framework of density functional theory (DFT). The effective core potential method is invoked to calculate these clusters in order to take consideration of remarkable inner electron relativistic effect of gold atom. The number of distinct initial geometries is important to the reliability of the obtained lowest-energy structures. In the present work, we choose the initial structures of gold clusters by two ways as follows: first, considering the configurations of the Au clusters available from the previous studies,[7−9] we optimized the equilibrium geometries of Au_n clusters. Second, the initial structure of Au_n is generated using a genetic algorithm (GA).[49] The GA is shown to be an effective way to produce a large number of isomers for further DFT optimizing. On the basis of the optimized pure gold clusters, we construct the initial configuration of Au_nAl by directly adding or substituting a Al atom. In all, the equilibrium geometries of Au_nAl clusters are optimized, and their stabilities are reassured accurately by the harmonic vibrational frequency calculation. Therefore, all isomers for this cluster are surely the local minima.

The geometries and electronic properties are quite sensitive to the exchange and correlation functional used in the DFT method. To test the quality of the PW91PW91/CEP-121G scheme for the description of the Au_nAl clusters, we analyse dimer in detail and show the results in Table 1. The exchange-correlation functional of the Slater exchange functional[50] and the Vosko–Wilk–Nusair correlational functional (SVWN5),[51] hybrid three parameter Becke (B_3) and Perdew and Wang's 1991 gradient-corrected correlation functional, hybrid three

Table 1. The binding energies (E_b), bond lengths (R_e), and vibrational frequencies (ω_e) of Au_2 and AuAl clusters at different levels.

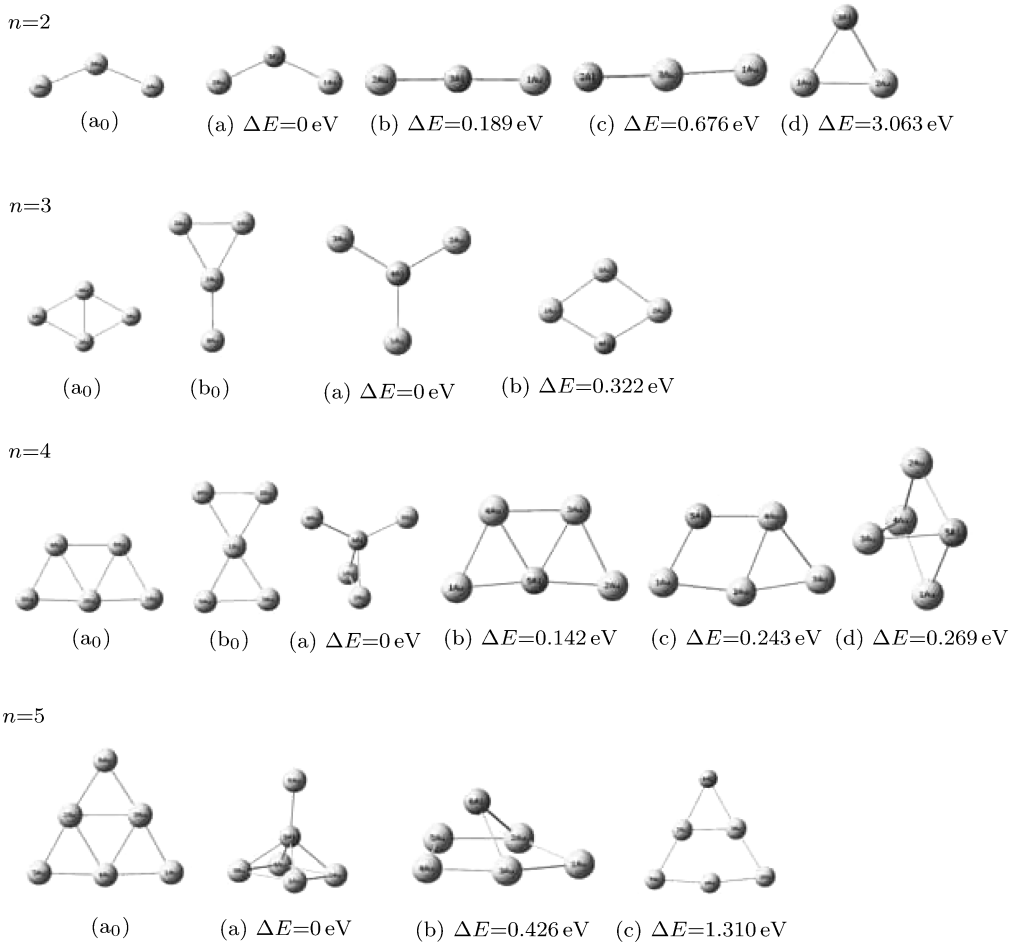
cluster	method	basis set	E_b/eV	R_e/Å	ω_e/cm^{-1}
Au_2	SVWN5	SDD	2.77	2.499	189
		CEP-121G	2.82	2.489	193
		LANL2DZ	2.78	2.490	193
	B3PW91	SDD	1.89	2.553	170
		CEP-121G	1.92	2.545	172
		LANL2DZ	1.90	2.546	171
	B3LYP	SDD	1.86	2.579	163
		CEP-121G	1.91	2.571	164
		LANL2DZ	1.87	2.573	162
	PW91PW91	SDD	2.19	2.556	168
		CEP-121G	2.25	2.546	170
		LANL2DZ	2.20	2.547	169
	experimental[17]		2.30	2.472	191
AuAl	SVWN5	SDD	4.03	2.395	329
		CEP-121G	3.89	2.430	317
		LANL2DZ	3.96	2.449	312
	B3PW91	SDD	3.05	2.440	304
		CEP-121G	2.95	2.460	297
		LANL2DZ	3.02	2.474	295
	B3LYP	SDD	3.06	2.455	294
		CEP-121G	2.95	2.470	290
		LANL2DZ	3.01	2.483	289
	PW91PW91	SDD	3.44	2.436	306
		CEP-121G	3.33	2.456	300
		LANL2DZ	3.38	2.469	298
	experimental[17,52]		3.34	2.339	333

parameter Becke (B_3) with Lee–Yang-Parr (LYP) correlation functional,[53] and the gradient corrected exchange and correction functional of Perdew and Wang (PW91PW91)[54] are investigated for Au_2 and AuAl clusters, respectively. The binding energies (E_b), bond lengths (R_e), and vibrational frequencies (ω_e) of Au_2 and AuAl are calculated by different functionals with three ECP basis sets (Table 1). Compared with theoretical and experimental calculations, the results from PW91PW91/CEP-121G are relatively closer to experiment than from other methods, although the bond length and the frequency have larger errors than the results of experiments. Furthermore, using this method, the calculated lowest-energy structure of Au_7 cluster is in excellent agreement with the experimental result.[54] Therefore, in this paper, the PW91PW91/CEP-121G method is used to study small Au_nAl clusters. All calculations are implemented with the Gaussian 03 program package.[55] The convergence criteria of optimization is set to 10^{-6} a.u. for energy gradient and atomic displacement.

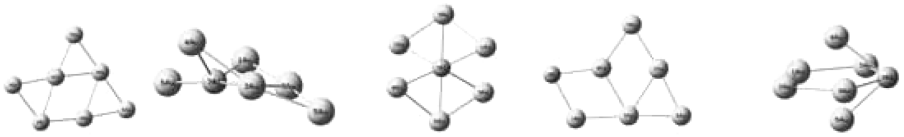
3. Results and discussion

3.1. Equilibrium geometry

In this work, we have studied Au_nAl at the PW91PW91/CEP-121G level by DFT. The lowest-energy structures and some low-lying isomers of Au_nAl are plotted in Fig.1. The isomers are labelled with two indices: the first one (number) represents the number of Au atoms in the cluster, and the second one (letter) ranks the isomer in the descending order of the binding energy. For comparison, the lowest-energy structures for pure Au_{n+1} clusters are also shown in Fig.1, which have been explored with the same computation scheme and agree well with previous theoretical results except for $n = 13$ and 14.[9]

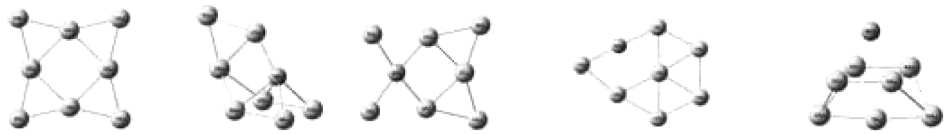


n=6



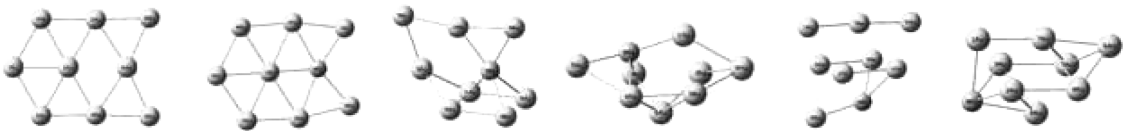
(a_0) (a) ΔE=0 eV (b) ΔE=0.187 eV (c) ΔE=0.438 eV (d) ΔE=0.564 eV

n=7



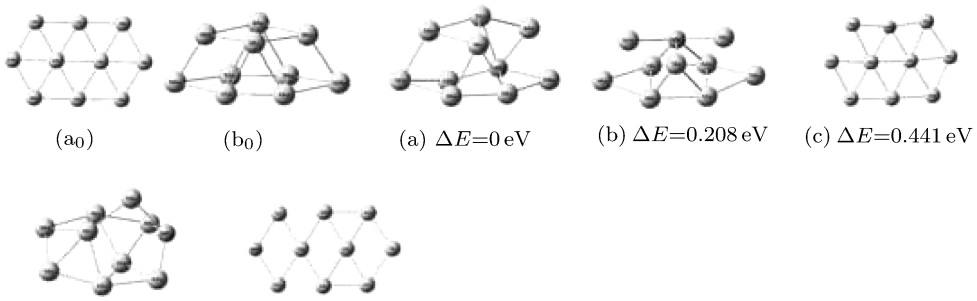
(a_0) (a) ΔE=0 eV (b) ΔE=0.392 eV (c) ΔE=0.501 eV (d) ΔE=1.260 eV

n=8



(a_0) (a) ΔE=0 eV (b) ΔE=0.224 eV (c) ΔE=0.301 eV (d) ΔE=0.394 eV (e) ΔE=1.141 eV

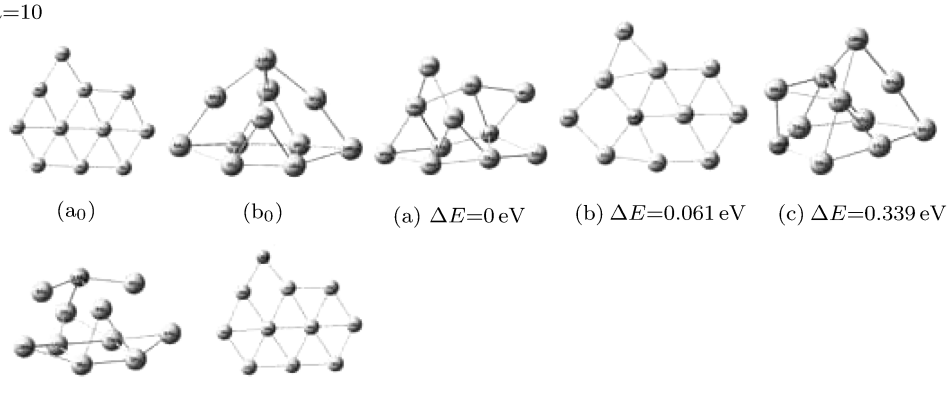
n=9



(a_0) (b_0) (a) ΔE=0 eV (b) ΔE=0.208 eV (c) ΔE=0.441 eV

(d) ΔE=0.495 eV (e) ΔE=1.010 eV

n=10



(a_0) (b_0) (a) ΔE=0 eV (b) ΔE=0.061 eV (c) ΔE=0.339 eV

(d) ΔE=0.353 eV (e) ΔE=0.732 eV

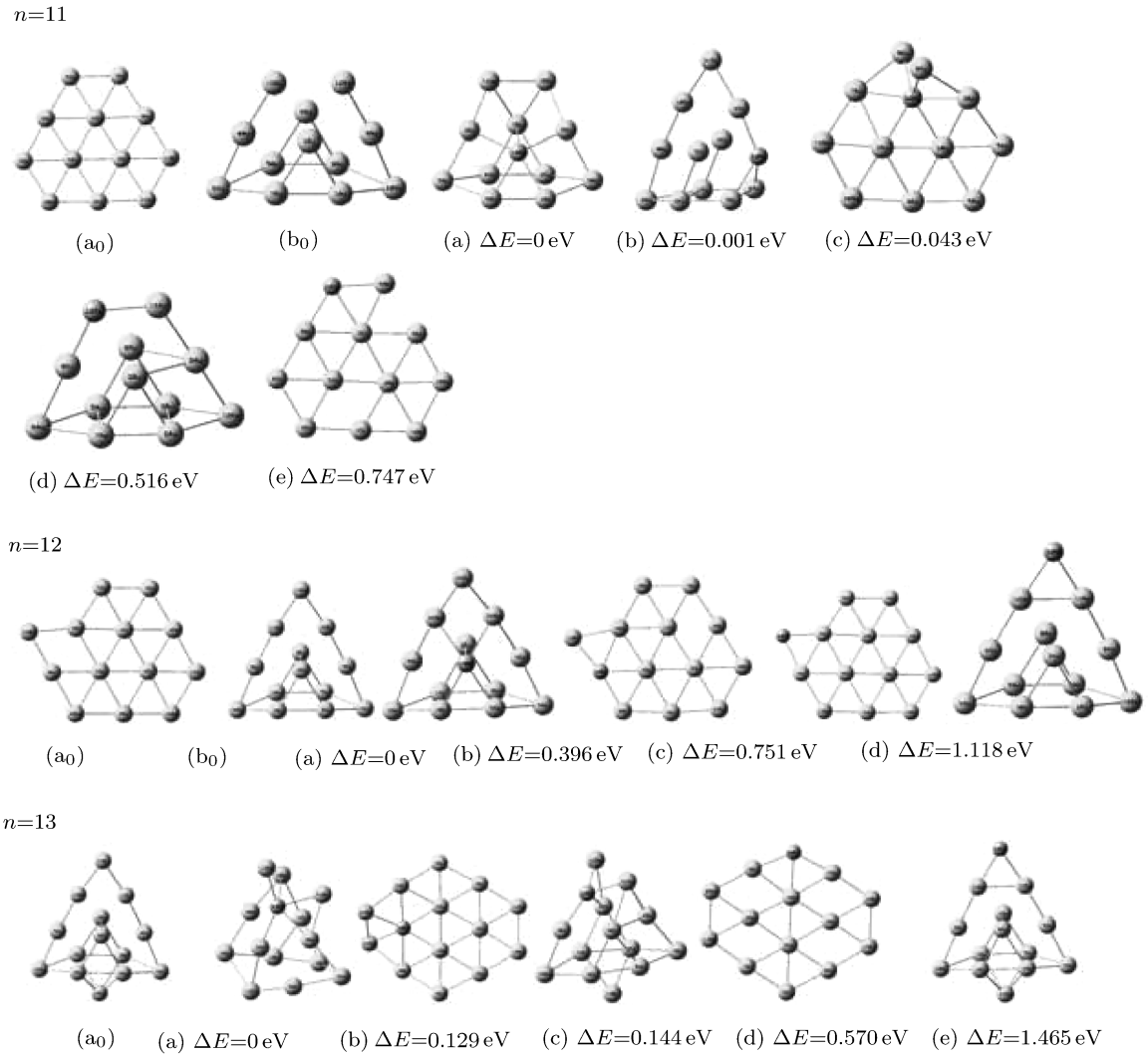


Fig.1. The lowest energy and low-lying structures of Au_nAl clusters and the lowest-energy structures of pure Au_{n+1} ($n = 2 - 13$) clusters.

The lowest-energy structure (2a in Fig.1) of Au_2Al cluster can be obtained by directly adding one Al atom to the pure Au_2 cluster. It is an isosceles triangle with an obtuse-angle, similar to that of Au_3 as shown in Fig.1. It is to be noted that the shortest Au–Al bond (2.419 Å) of Au_2Al is weakened compared to the shortest Au–Au distance (2.590 Å) of Au_3. The other three isomers of Au_2Al are two linear and one isosceles structures. The energy difference between these isomers and its lowest-energy structure are 0.189 eV, 0.676 eV, and 3.063 eV, respectively.

The lowest-energy structure of Au_3Al cluster (3a in Fig.1) can be obtained by substituting one Al atom for one Au atom from the low-lying Y-shaped isomer of the Au_4 cluster ($3b_0$ in Fig.1). It is different from the lowest-energy structure of the Au_4 cluster ($3a_0$ in Fig.1). The lowest-energy structure of Au_4 is a rhombus configuration, in agreement with previous calculations.[7–9] But the distorted rhombus structure of Au_3Al (3b in Fig.1) is found to be 0.322 eV higher in energy than the lowest-energy geometry.

For Au_nAl clusters, the first important structural change occurs at $n = 4$. From Au_4Al to Au_7Al clusters, the lowest-energy structures are all found to be non-planar, different from those of the pure Au_{n+1} ($4 \leq n \leq 7$) clusters. The lowest-energy configuration of the Au_4Al cluster (4a in Fig.1) can be obtained by substituting one Al atom for one Au atom in the X-shaped structure of the pure Au_5 cluster ($4b_0$ in Fig.1). The planar M-shaped structure of Au_4Al is 0.142 eV higher in energy than its lowest-energy configuration.

The lowest-energy structure of Au_5Al cluster (5a in Fig.1) can be obtained by changing the site of a Au atom on the low-lying structure of Au_5Al cluster (5b in Fig.1), which is a capped foursquare pyramid with four

Au bases, an Al apex and an Au cap. The next isomer is higher in energy (ΔE=0.426 eV) than this structure. It should be mentioned that the results are in agreement with ones of Majumder *et al.*[38] Furthermore, the planar structure is significantly higher in energy than the lowest-energy structure by 1.310 eV.

For the Au_6Al cluster, the lowest-energy structure (6a in Fig.1) is obtained by substituting one Al atom for one Au atom from the Au_7 cluster, which is a capped triangle configuration. Two planar isomers of Au_6Al cluster are slightly higher by 0.187 eV and 0.438 eV in total energy, respectively. Among 3D structures, the pentagonal bipyramid is higher in energy than the lowest-energy structure ($\Delta E = 0.564$ eV).

The lowest-energy structure of Au_7Al can be obtained by adding an Au atom in one of the Au_6Al clusters (7a in Fig.1). The other three low-lying isomers (7b, 7c and 7d in Fig.1) are substitutional structures of Au_8 cluster and are higher in energy than the 7a by 0.392, 0.501 and 1.260 eV, respectively.

The next important structural change occurs for the Au_8Al cluster, which favours a planar geometry. The lowest-energy structure of Au_8Al cluster (8a in Fig.1) can be obtained by substituting one Al for one Au atom from one of the Au_9 clusters as shown in Fig.1. Both of the Au_8Al and Au_9 clusters are di-edge-bridged hexagon configurations with different bond length. Several possible nine-vertex geometries of 3D structures including the capped pyramid and tetra-capped tetrahedron *et al* are all studied. All of the 3D structures are higher in energy than the lowest-energy structure by 0.224, 0.301, 0.394 and 1.141 eV, respectively.

All of the Au_9Al to $Au_{13}Al$ clusters still prefer non-planar structures, different from those of the pure Au_{n+1} ($9 \leq n \leq 13$) (shown in Fig.1). For Au_9Al clusters, a 3D structure (9a in Fig.1) is found to be lowest in energy, which is obtained by substituting one Al atom for one Au atom from the low-lying isomer of the Au_{10} cluster ($9b_0$ in Fig.1). Several possible geometries obtained by adding Al atom to the isomers of Au_9 cluster are investigated but were found to be at least 0.208 eV higher in energy.

For $Au_{10}Al$ clusters, several isomeric structures were calculated. The lowest-energy configuration can be obtained by substituting one Al atom for Au from the low-lying structure of the Au_{11} clusters ($10b_0$ in Fig.1). The planar geometry (10b in Fig.1) from the lowest energy structure of Au_{11} is higher in energy than the lowest-energy state by 0.061 eV.

By preferring 3D configuration, $Au_{11}Al$ follows the same trend as that of $Au_{10}Al$. The lowest-energy configuration can be obtained by substituting an Al atom for one Au from the low-lying structure of the Au_{12} clusters ($11b_0$ in Fig.1). But the structure (11b in Fig.1) is slightly higher than this lowest-energy configuration in energy by 0.001 eV. This may be because both structures come from the same configuration of Au_{12} cluster.

We perform an extensive computational search for the global minimum structure of $Au_{12}Al$ and find that the lowest-energy configuration (12a in Fig.1) is obtained by substituting one Al atom for Au from the low-lying structure of the Au_{13} clusters ($12b_0$ in Fig.1). Three metastable isomers are shown in Fig.1 in 12b–12d and these isomers are higher in energy than the lowest-energy state by 0.396, 0.751, and 1.118 eV, respectively.

The biggest cluster studied in this work is the $Au_{13}Al$ cluster. The lowest-energy structure of $Au_{13}Al$ (13a in Fig.1) can be obtained by adding one Au atom in the lowest-energy configuration of $Au_{12}Al$. The binding energy of the lowest-energy structure is the 2.250 eV/atom, which is the only higher 0.028 eV/atom than the next isomer (13b in Fig.1). It is to be noted that the lowest-energy structures of Au_{13} and Au_{14} clusters are three-dimensionally different from the planar configurations of Au_{n+1} ($2 \leq n \leq 12$).[9]

According to the discussion above, it is concluded that the lowest-energy structures of Au_nAl clusters can be obtained by adding one Au atom or substituting one Au atom in the interior or peripheral site of the pure gold clusters. From $n = 2$ to $n = 8$, the lowest-energy structures of Au_nAl clusters can be described as an Al atom prefering the endo-site of the Au_{n+1} clusters. From $n = 9$ to $n = 13$, the lowest-energy structures of Au_nAl clusters can be described as an Al atom occupying the peripheral site of the Au_{n+1} clusters. For the Au_nAl clusters, except for Au_8Al, the turnover point from two-dimensional to three-dimensional geometry occurs at n=4, which is different from the ones of Au_nS, Au_nTi, Au_nCu and Au_nSi ($n = 6$, $n = 8$, $n = 5$ and $n = 3$, respectively).[33,34,38,39]

3.2. Relative stability

In order to analyze the stability of Au_nAl, we have calculated their average binding energies. The average binding energies for the Au_nAl clusters can be defined as the following formula: $E_b(Au_nAl)=[nE(Au)+E(Al)-E(Au_nAl)]/(n+1)$, where $E(Au)$, $E(Al)$, and $E(Au_nAl)$ represent the total energies of the most stable Au, Al, and Au_nAl clusters, respectively.

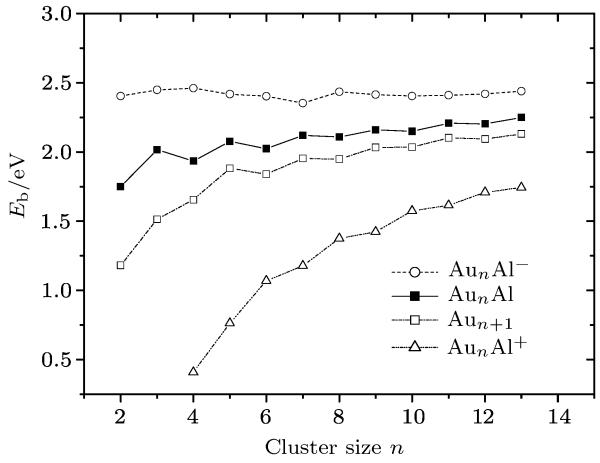


Fig.2. Size dependence of the binding energy per atom (E_b) of neutral, ionic Au_nAl and Au_{n+1} ($n = 2-13$) clusters.

The binding energy per atom for Au_nAl neutral and ionic clusters against the number of atoms is shown in Fig.2. For comparison, we have also plotted the binding energy per atom for Au_{n+1} clusters, which clearly indicates that the substitution of the Au atom by Al enhances the binding energy of the given clusters. This is due to the lower bond length of the Au–Al (2.455 Å) than Au–Au (2.546 Å). The binding energy of Au_nAl reveals the even-odd effect with enhanced stability at odd-numbered clusters, which is consistent with the tendency of Au_{n+1}. For Al doped clusters, the average binding energy increases substantially as compared with the binding energy of the host cluster, but finally tends to saturate. The average binding energy curves for anionic and cationic clusters show a different nature as that of the neutral, which does have not obvious even-odd effect. As shown in Fig.2, an addition of one electron increases the Au–Al interaction by decreasing the Au–Al bond lengths in anionic clusters. This will enhance the binding energy of Au_nAl^- as compared with a neutral one as well as compared with the host clusters. However, the removal of electron decreases the Au–Al interaction, which results in less stability for the cationic clusters.

The stability of these clusters is also analysed by examining fragmentation energies. Here, we consider two fragmentation channels involving either an Au atom or an Al atom. The fragmentation energies for a neutral Au_nAl cluster are calculated as $\Delta^1E(Au_nAl)=E(Au_nAl)-[E(Au_n)+E(Al)]$, $\Delta^2E(Au_nAl)=E(Au_nAl)-[E(Au_{n-1}Al)+E(Au)]$, where E is the total energy of the system.

Figure 3 shows the fragmentation energies for the Au_nAl clusters with respect to Au and Al atoms. Δ^1 is the energy gain in adding an Al atom to Au_n clusters, and Δ^2 is the energy gain in adding an Au atom to an $Au_{n-1}Al$ cluster. It is found that the interaction of the Al atom with the Au_n clusters is energetically more favorable than the Au atom, which is in agreement with the lower bond length of Au–Al than Au–Au. For Al induced clusters, the energetically lowest fragmentation channel is the lowest 2.01 eV for Au_4Al cluster. These behaviours of Δ^1 and Δ^2, and more precisely, $\Delta^1 \gg \Delta^2$ for all n, indicate that the addition of Al to an Au cluster is energetically favorable. It is to be noted that the curves has obvious odd–even change, which is consistent with the change tendency in binding energy.

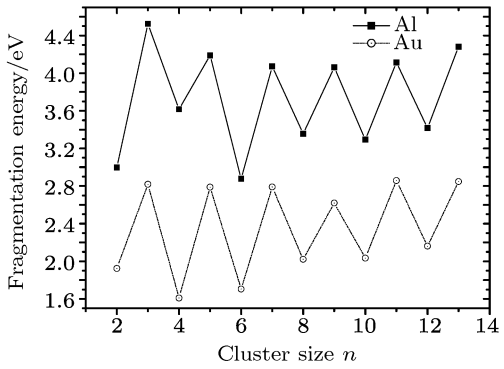


Fig.3. Size dependence of the fragmentation energy (eV)) of Au_nAl ($n = 2-13$) clusters via loss of a Al atom and a Au atom.

3.3. Electronic properties

The highest-occupied molecular orbital (HOMO) and the lowest-unoccupied molecular orbital (LUMO) gap, having relations with the relative chemical reactivity of clusters, is of much importance in theoretical researches. It is found that systems with larger HOMO–LUMO gap are less reactive. In our work, the HOMO–LUMO gaps of the lowest-energy structures of Au_nAl and Au_{n+1} clusters are calculated, and the results are displayed in Fig.4. As shown in Fig.4, the HOMO–LUMO gaps of Au_nAl are usually larger than

those of Au_{n+1} clusters except at $n = 5$ and 10. The gaps are close to each other at $n = 5$, 7, 9, 11, 13 and 2, 4, 6, 8, 10, 12, respectively. There is a maximum at Au_3Al (2.372 eV) and a sharp minimum at $Au_{10}Al$ (0.177 eV). There is an obvious odd–even oscillation between the size number and the gap of Au_nAl. It is consistent with the change of Au_{n+1} cluster on gaps.

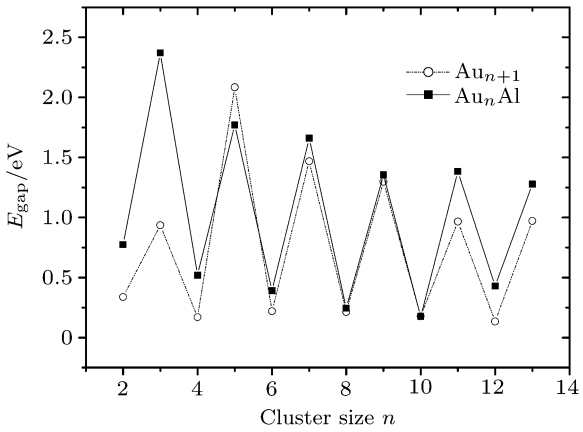


Fig.4. Size dependence of the HOMO–LUMO gap (E_{gap}) of Au_nAl and Au_{n+1} ($n = 2 - 13$) clusters.

The vertical ionization potential (VIP) is an important parameter to understand the chemical stability toward ejecting out one electron from its HOMO energy level to the continuum. The larger the VIP, the deeper the HOMO energy level, which leads to less reactivity or higher chemical stability. In this work, the VIPs of Au_nAl and Au_{n+1} clusters are calculated and shown in Fig.5. For Au_nAl clusters, the odd n have larger vertical ionization potential, corresponding to their higher stability. The Au_{n+1} clusters with odd n were found to have larger vertical ionization except for $n = 2$, which is in agreement with previous results.[9] In addition, there is the same trend

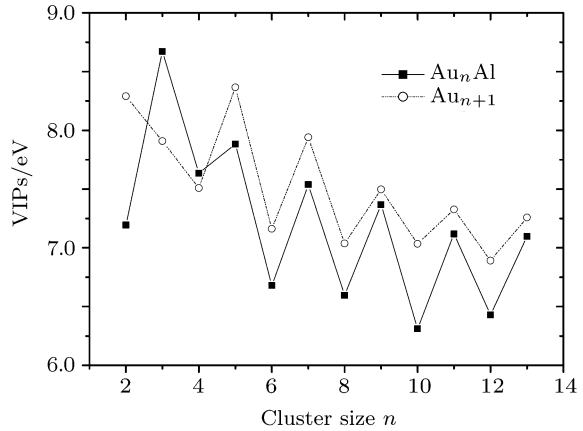


Fig.5. Size dependence of the vertical ionization potentials (VIPs) of Au_nAl and Au_{n+1} ($n = 2 - 13$) clusters.

for Au_nAl and Au_{n+1} the vertical ionization potential generally decreases with cluster size. A distinct phenomena for Au_nAl clusters is that n=3 has a higher vertical ionization potential than the others, which is attributed to its stable structure. $Au_{10}Al$ has the smallest VIP (6.312 eV), in agreement with the previous experimental result.[44]

Electron affinity (EA) is an important parameter to understand the stability of cluster. In this work, the EAs of Au_nAl and Au_{n+1} clusters for their lowest-energy structures are calculated and shown in Fig.6. The Au_nAl clusters with odd n are found to have lower EAs than even n. The data of Au_{n+1} clusters has the same tendency. However, Au_3Al cluster has the lowest EA (1.729 eV), corresponding to the highest stability. From Fig.6, we can see EAs of Au_nAl are all lower than those of Au_{n+1}. In addition, there is a trend for Au_nAl and Au_{n+1} that the EAs generally increases with cluster size.

Though the doping of Al atom enhances the chemical stabilities of gold clusters, it does not change the variational trend of the electronic properties. In the Periodic Table, the valance electrons for the Au and the Al atoms will be [core]$5d^{10}6s^1$ and [core]$3S^2 3p^1$, respectively. They have only one s-valance electron and one p-valance electron, respectively. The experiments have found that these clusters with one valance electron have the same even–odd effect.[56,57]

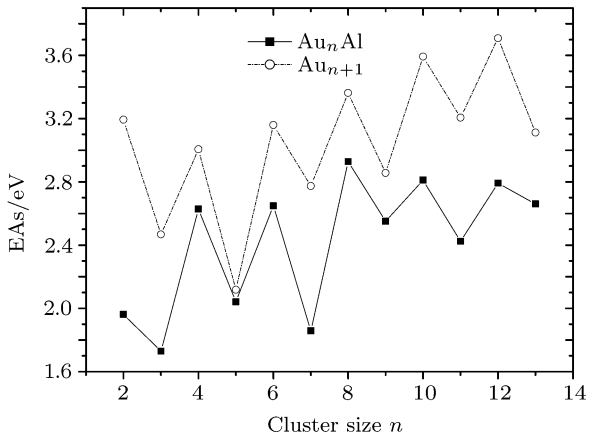


Fig.6. Size dependence of the electron affinities (EAs) of Au_nAl and Au_{n+1} ($n = 2 - 13$) clusters.

3.4. Natural bonding orbital analysis

In order to understand the bonding nature in these AuAl bimetallic clusters, we have studied the natural bond orbital analysis[58] at their lowest-energy geometries. The natural electron configurations for

each of the atoms in the case of the Au_2, Al_2 and AuAl dimers are provided in Table 2. In Table 2. Au_2 and Al_2 dimers have the natural electron configuration of $[core]6S^{1.05}5d^{9.94}6p^{0.01}$ and $[core]3S^{1.98}3p^{1.02}$ at each of the Au and Al atoms respectively. In the CEP-121G basis set the valance electrons for the Au and Al atoms will be $[core]5d^{10}6s^1$ and $[core]3S^23p^1$, respectively. From Table 2, it is evident that few electron transfer occurs in both Au and Al dimers. Whereas in the case of the AuAl dimer, a partial charge transfer is found to occur, in which about 0.5 electron is transferred from the 3p orbital of Al to the 6s orbital of Au atom. This is primarily related to the differing Pauling's electronegativity of Au and Al atoms. The order of magnitude of their electronegativity is Au (2.54)>Al (1.61). It is notable that there are large amounts of charge transformations in AuAl due to the difference of electronegativity between the Au and the Al atoms.

Table 2. The natural electron configuration of Au_2, Al_2, and AuAl dimer in their lowest-energy states structures.

cluster	atom number	natural electron configuration
Au_2	Au(1)	$[core]6s^{1.05}5d^{9.94}6p^{0.01}$
	Au(2)	$[core]6s^{1.05}5d^{9.94}6p^{0.01}$
Al_2	Al(1)	$[core]3s^{1.98}3p^{1.02}$
	Al(2)	$[core]3s^{1.98}3p^{1.02}$
AuAl	Au(1)	$[core]6s^{1.63}5d^{9.86}7s^{0.01}7p^{0.01}$
	Al(1)	$[core]3s^{1.96}3p^{0.53}$

4. Conclusions

we have studied equilibrium geometries and electronic properties of Au_nAl and Au_{n+1} clusters using the density functional theory. For Au_nAl (n = 2, 3 and 8) clusters, the lowest energy structures favour planar structure. From $n = 4$ to $n = 13$, except for $n = 8$, the lowest-energy structures of Au_nAl clusters favour 3D structures. Those structures are obtained by substituting one Au by Al atom from Au_{n+1} clusters as well as by placing the Au atom on each possible site of the $Au_{n-1}Al$ clusters. Furthermore, the stabilities of Au_nAl clusters present obvious even/odd alternations phenomenon and the Au_nAl clusters with odd n are more stable than those with even n, which are in agrement with the case of Au_{n+1} clusters. we find the same trend of alternation in the HOMO–LUMO gap, the vertical ionization potential and the electron affinities. Though the doping Al atom does not influence this even/odd alteration, it changes the structures of free gold clusters and enhances their stabilities. Finally, we study the natural bond orbital analysis of Au_nAl clusters at their lowest-energy geometries. The results show about 0.5 electron transfers from the 3p orbital of Al to the 6s orbital of Au atom.

References

[1] Schwerdtfeger P 2003 *Angew. Chem. Int. Ed.* **43** 1892

[2] Daniel M C and Astruc D 2004 *Chem. Rev.* **104** 293

[3] Pyykkö P 2004 *Angew. Chem. Int. Ed.* **43** 4412

[4] Pyykkö P 2005 *Inorg. Chim. Acta* **358** 4113

[5] Mao H P, Wang H Y, Ni Y, Xu G L, Ma M Z, Zhu Z H and Tang Y J 2004 *Acta Phys. Sin.* **53** 1766 (in Chinese)

[6] Bulusu S and Zeng X C 2006 *J. Chem. Phys.* **125** 154303

[7] Xiao L, Tollberg B, Hu X and Wang L 2006 *J. Chem. Phys.* **124** 114309

[8] Idrobo J C, Walkosz W, Yip S F, Öğüt S, Wang J and Jellinek J 2007 *Phys. Rev.* B **76** 205422

[9] Li X B, Wang H Y, Yang X D and Zhu Z H 2007 *J. Chem. Phys.* **126** 084505

[10] Wilson N T and Johnston R L 2002 *Eur. Phys. J.* D **12** 161

[11] Furche F, Ahlrich R, Weis P, Jacob C, Gilb S, Bienweiler T and Kappes M 2002 *J. Chem. Phys.* **117** 6982

[12] Dietrich G, Krückeberg S, Lützenkirchen K, Schweikhard L and Walther C 2000 *J. Chem. Phys.* **112** 752

[13] Rousseau R and Marx D 2000 *J. Chem. Phys.* **112** 761

[14] Zhang Z, Berg A, Levanon H, Fessenden R and Meisel W D 2003 *J. Am. Chem. Soc.* **125** 7959

[15] Gilb S, Weis P, Furche F, Ahlrichs R and Kappes M M 2002 *J. Chem. Phys.* **116** 4094

[16] Wang J, Wang G and Zhao J 2003 *Chem. Phys. Lett.* **380** 716
[17] Huber K P and Herzberg G 1979 *Constants of Diatomic Molecules* (New York: van Nostrand Reinhold)
[18] Barnett R N, Cleveland C I, Häkkinen H, Luedtke W D, Yamouleas C and Landsman U 1999 *Eur. Phys. J.* D **9** 95
[19] Koyasu K, Mitsui M, Nakajima A and Kaya K 2002 *Chem. Phys. Lett.* **358** 224
[20] Mao H P, Sheng Y and Wang H Y 2008 *Chin. Phys.* B **17** 2110
[21] Mao H P, Wang H Y, Zhu Z Y and Tang Y J 2006 *Acta Phys. Sin.* **55** 4542 (in Chinese)
[22] Wang H Y, Li X B, Tang Y J, Chen X H, Wang C Y and Zhu Z H 2005 *Acta Phys. Sin.* **54** 3565 (in Chinese)
[23] Li Q and Zhu Z H 2008 *Acta Phys. Sin.* **57** 3419 (in Chinese)
[24] Zhao L X, Cao T T, Feng X J, Liang X, Lei Y M and Luo Y H 2008 *J. Mol. Struct.* (THEOCHEM) **895** 92
[25] Häkkinen H, Abbet S, Sanchez A, Heiz U and Landman U 2003 *Angew. Chem., Int. Ed.* **42** 1297
[26] Tanaka H, Neukermans S, Janssens E, Silverans R E and Lievens P 2003 *J. Am. Chem. Soc.* **125** 2862
[27] Wang S Y, Yu J Z, Mizuseki H, Sun Q, Wang C Y and Kawazoe Y 2004 *Phys. Rev.* B **70** 165413
[28] Torres M B, Fernandez E M and Balbas L C 2005 *Phys. Rev.* B **71** 155412
[29] Pyykkö P and Runeberg N 2002 *Angew. Chem. Int. Ed.* **41** 2174
[30] Li X, Kiran B, Li J, Zhai H J and Wang L S 2002 *Angew. Chem. Int. Ed.* **41** 4786
[31] Neukermans S, Janssens E, Tanaka H, Silverans R E and Lievens P 2003 *Phys. Rev. Lett.* **90** 033401
[32] Janssens E, Tanaka H, Neukermans S, Silverans R E and Lievens P 2004 *Phys. Rev.* B **69** 085402
[33] Gao Y, Bulusu S and Zeng X C 2005 *J. Am. Chem. Soc.* **127** 15680
[34] Janssens E, Neukermans S, Nguyen H M T, Nguyen M T and Lievens P 2005 *Phys. Rev. Lett.* **94** 113401
[35] Janssens E, Neukermans S, Wang X, Veldeman N, Silverans R E and Lievens P 2005 *Eur. Phys. J.* D **34** 23
[36] Li X, Kiran B, Cui L F and Wang L S 2005 *Phys. Rev. Lett.* **95** 253401
[37] Sahu B R, Maofa G and Kleinman L 2003 *Phys. Rev.* B **67** 115420
[38] Majumder C 2007 *Phys. Rev.* B **75** 235409
[39] Majumder C and Kulshreshtha S K 2007 *Phys. Rev.* B **127** 214706
[40] Yuan D W, Wang Y and Zeng Z 2005 *J. Chem. Phys.* **122** 114310
[41] Chen M X and Yan X H 2008 *J. Chem. Phys.* **128** 174305
[42] Wang H Y, Li X B, Tang Y J, King R B and Schaefer III H F 2007 *Chin. Phys.* **16** 1660
[43] Bouwen W, Vanhoutte F, Despa F, Bouckaert S, Neukermans S, Kuhn L T, Weidele H, Lievens P and Silverans R E 1999 *Chem. Phys. Lett.* **314** 227
[44] Heinebrodt M, Malinowski N, Tast F, Branz W, Billas I M L, and Martin T P 1999 *J. Chem. Phys.* **110** 20
[45] Majumder C, Kandalam A K and Jena P 2006 *Phys. Rev.* B **74** 205437
[46] Perdew J P, Burke K and Wang Y 1996 *Phys. Rev.* B **54** 16533
[47] Cundari T R and Stevens W J 1993 *J. Chem. Phys.* **98** 5555
[48] Kohn W and Shan L J 1965 *Phys. Rev.* A **140** 1133
[49] Ercolessi F, Parrinello M and Tosatti E 1988 *Philos. Mag.* A **58** 213
[50] Slater J C 1974 *Quantum Theory of Molecules and Solid* (New York: McGraw-Hill)
[51] Vosko S J, Wilk L and Nusair M 1980 *Can. J. Phys.* **58** 1200
[52] Gingerich K A and Blue G D 1973 *J. Chem. Phys.* **59** 185
[53] Lee C, Yang W and Parr R G 1998 *Phys. Rev.* B **37** 785
[54] Gruene P, Rayner D M, Redlich B, van der Meer A F G, Lyon J T, Meijer G and Fielicke A 2008 *Science* **321** 674
[55] Frisch M J, Trucks G M, Schlegel H B, Scuseria G E, Robb M A, Cheeseman J R, Montgomery J A, Vreven T, Kudin K N, Burant J C, Millam J M, Iyengar S S, Tomasi J, Barone V, Mennucci B, Cossi M, Scalmani G, Rega N, Petersson G A, Nakatsuji H, Kitao O, Nakai H, Klene M, Li X, Knox J E, Hratchian H P, Cross J B, Adamo C, Jaramillo J, Gomperts R, Stratmann R E, Yazyev O, Austin A J, Cammi R, Pomelli C, Ochterski J W, Ayala P Y, Morokuma K, Voth G A,Salvador P, Dannenberg J J, Zakrzewski V G, Dapprich S, Daniels A D, Strain M C, Farkas O, Malick D K, Rabuck A D, Raghavachari K, Foresman J B, Ortiz J V, Cui Q, Baboul A G, Clifford S, Cioslowski J, Stefanov B B, Liu G, Liashenko A, Piskorz P, Komaromi I, Martin R L, Fox D J, Keith T, Al-Laham M A, Peng C Y, Nanayakkara A, Challacombe M, Gill P M W, Johnson B G, Chen W, Wang M W, Gonzales C and Pople J A 2003 Gaussian 03 (Revision C.02) (Pittsburgh, PA: Gaussian Inc.)
[56] Joyes P and Sudrand P 1985 *Surf. Sci.* **156** 451
[57] Satter K 1981 *Phys. Rev. Lett.* **47** 160
[58] Reed A E, Curtiss L A and Weinhold F 1988 *Chem. Rev.* **88** 899